Thesis for Master Degree

Regulation of PLIN5 Gene Expression by LRH-1 in the Liver

Graduate School, Keimyung University

School of Medicine

Pantha, Rubee

Supervisor Im, Seung Soon

February, 2021

Regulation of PLIN5 Gene Expression by LRH-1 in the Liver

Supervisor Im, Seung Soon

A Thesis Submitted for Master's Degree

February, 2021

Graduate School, Keimyung University

Department of Physiology

Pantha, Rubee

Pantha, Rubee's Master Thesis is Approved

Committee Chair Bae, Jae Hoon

Committee Member Im, Seung Soon

Committee Member Song, Dae Kyu

Graduate School, Keimyung University

February, 2021

Acknowledgement

I would like to express my profound gratitude and immeasurable thanks to my supervisor, professor Im, Seung Soon, for his supervision, guidance, support, encouragement and motivation. His friendly guidance and valuable advice have been invaluable to achieve my goals. Furthermore, I am blessed to get him as my advisor, who is kind-hearted, loving and caring person indeed. Also, I would like to express my gratitude to Professor Bae, Jae Hoon and Song, Dae Kyu for their valuable comments, extended discussions and suggestions which helped greatly for the improvement of my research.

I am very thankful to all my lab members including Dr. Lee, Jae Ho, Mr. Kim, Do-Young and Jang, Hye Ji for their help, support and co-operation. Additionally, I can't withstand without my sincere gratitude to my husband Mr. Bashyal, Santosh, who supported and encouraged me to persue my master's degree. I am very thankful for his motivational words during my hard time. I would also like to acknowledge all the faculty members and staff of School of Medicine, Keimyung University. I am very thankful to all who contributed directly and indirectly for the completion of my thesis. Last but not the least, I would like to express my deepest gratitude to my parents, parents-in-law and family members in Nepal for their love, moral support and best wishes to accomplish my work.

February, 2021

Pantha, Rubee

Table of Contents

List of Table

List of Figures

1. Introduction

Liver receptor homolog-1 (LRH-1) is a representative of nuclear receptor 5A subfamily of orphan nuclear receptors, mainly expressed in the liver, pancreas, ovary and intestine (1,2). It is the principal regulator of glucose, bile acid and cholesterol metabolism with varied biological roles extending from regulation of cell cycle to the maintenance of steroid homeostasis (3,4). In the pancreas, LRH-1 with pancreas transcription factor stimulates the expression of genes encoding for pancreatic digestive enzymes and secretory proteins (5). Moreover, LRH-1 regulates maturation of ovarian follicles and ovulation in the ovary (6) and is responsible for mitochondrial function via regulation of cytochrome p450, familly 11, subfamily a, polypeptide 1 and cytochrome p450, familly 11, subfamily b, polypeptide 1 in intestinal epithelium (7). In the liver, LRH-1 is involved in the mitochondrial biogenesis and β-oxidation through regulation of peroxisome proliferator-activated receptor gamma coactivator 1-alpha gene expression (8). In addition, LRH-1 liver-specific knockout (LKO) mice show endoplasmic reticulum stress-induced fatty liver, indicating that LRH-1 plays a major role in triglycerides (TGs) accumulation in the liver (9).

Excess TGs in the liver are mainly reserved within the lipid droplet (LDs) (10). LDs are assigned for balancing lipid storage and utilization, and are strongly regulated in a cell type-specific manner (11). LDs modulate low intracellular free fatty acids levels and play a crucial role in protecting liver from lipotoxicity caused by excess fatty acids in nutritional stress conditions (10,12). In addition, the mobilization of LDs reflects the metabolic state of cells and also indicates changes in the LD-related proteins that contribute to the regulation of lipid metabolism

and lipid homeostatsis (13).

The perilipin (PLIN) protein family, which attaches to LDs, is a representative group of LD-associated proteins that utilizes the stored lipids of LDs via lipolysis (10,11). It is composed of five members, named PLIN1-5 and is classified based on stability in free state. PLIN1 and PLIN2 rapidly degrade in free state however, they exist when bound to LDs. The remaining proteins from the family, PLIN3, PLIN4 and PLIN5 are found either free in the cytosol or lining with the LDs (14). PLIN1 is reserved in brown adipose tissue (BAT), whereas PLIN2 and PLIN3 are distributed in many cell types, and PLIN2 is especially found in hepatocytes. PLIN4 is expressed in cardiomyocytes, adipocytes and myocytes, and PLIN5 is usually confined within tissues or cells with high oxidative capacity namely the liver, heart, BAT and muscle (11,14,15).

Among the PLIN family, PLIN5 has emerged as indispensable for adjusting lipid abundance. It is highly active upon fatty acid treatment in cultured cells, with high fat diet and upon prolonged fasting (10). Prolonged fasting is also known to increase TGs accumulation in the liver (16,17) due to increased adipose tissue lipolysis (18). Therefore, PLIN5 is also regarded as the regulator of TGs metabolism (19). The overexpression of PLIN5 in cells enhances the expression of genes encoding proteins involved in aerobic catabolism and promotes both TGs storage as well as fatty acid oxidation. Thus, PLIN5 rapidly mobilizes the energy by sensing the nutrient demand (20).

The orphan nuclear receptor LRH-1 is activated during nutritional stress and is involved in protecting liver from lipid overload by increasing the β-oxidation. Even though LRH-1 regulates mitochondrial biogenesis and lipid metabolism, its regulatory mechanism is not clear and function of LRH-1 under nutritional deprivation conditions has not

been completely addressed. Therefore, in this study, the regulatory function of LRH-1 was investigated during a nutrient deprivation state and PLIN5 was identified as a direct target of LRH-1 by utilizing the wild type (WT) and LRH-1 LKO mice. Herein, LRH-1 was observed to be a key player in controlling the lipid overload to maintain normal hepatic TGs. Taken together, this study suggests that LRH-1 enhances the β-oxidation to meet the cellular energy demand and increases TGs secretion in the bloodstream as well as protects the liver from lipid overload during nutritional stress induced by fasting.

2. Materials and Methods

2.1. Animal Studies:

Eight to twelve week-old WT and LRH-1 LKO mice were used for this study. Mice were housed in an specific pathogen free facility and fed a standard chow diet and water *ad libitum*. All animal experiments were performed following the guidelines provided by the Institutional Animal Care and Use Committee of Keimyung University (KM-2020-12R1).

2.2. Cell Culture:

HepG2 immortalized human hepatocytes and human embryonic kidney (HEK)-293T cells were cultured in Dulbecco's modified Eagle's medium (DMEM, Hyclone, Logan, UT, USA) supplemented with 10% fetal bovine serum (FBS, Hyclone) and 100 U/ml penicillin-streptomycin (P/S) as complete media. For LRH-1 agonist treatment, HepG2 cells were cultured in the presence or absence of 100 μM dialauroylphosphatidylcholine (DLPC, Sigma-Aldrich, Co., St. Louis, MO, USA) in DMEM complete media for 24 h. Primary hepatocytes were cultured in either William's Medium E (Gibco, Grand Island, NY, USA) supplemented with 10% FBS, 1% glutamax (Gibco) and 100 U/ml P/S or DMEM media supplemented with 10% FBS and 100 U/ml P/S. Cells were incubated in a humidified atmosphere containing 5% CO_2 at 37 ℃.

2.3. Quantitative Polymerase Chain Reaction (qPCR):

Total RNA was isolated from the liver sample of 24 h-fasted and fed WT and LRH-1 LKO mice as well as from HepG2 cells treated with a LRH-1 agonist, DLPC using TriZol reagent (Life Technologies, Carlsbad, CA, USA). cDNA was generated using iScript cDNA synthesis kit (Bio-Rad, Hercules, CA, USA) following manufacturers' instructions. The qPCR was performed using a CFX96^{TM} real time system (Bio-Rad) to measure the expression level of various genes (Table 1). The relative mRNA expression level was normalized to ribosomal protein L32 or ribosomal phosphoprotein P0 by calculating with delta-delta threshold cycle method.

2.4. Western Blot Analysis:

Protein samples were collected from the liver tissues of fed and fasted WT and LRH-1 LKO mice as well as from a LRH-1 agonist-treated HepG2 cells. The tissues were homogenized in tissue lysis buffer (T-PER^{TM} tissue protein extraction reagent, Thermo Scientific, Rockford, IL, USA) supplemented with the complete mixture of protease inhibitors. Alike, cells were collected and resuspended in RIPA lysis buffer with protease inhibitors cocktail. Equal concentrations of proteins along with loading dye were incubated at 94 ℃ for 5 min and separated by the aid of sodium dodecyl sulfate-polyacrylamide gel electrophoresis. Subsequently, separated proteins were electroblotted onto nitrocellulose membranes (GE Healthcare, Uppsala, Sweden) followed by blocking with 5% non-fat milk. Then, blocked membrane was incubated overnight at 4 ℃ with anti-LRH-1 (ARP37407_P050) from Aviva System Biology (San Diego, CA, USA), anti-PLIN5 (PA1-46215) from Invitrogen (Carlsbad, California, USA), anti-CPT-1α (sc-393070), anti-PPARα (sc-398394) and

anti-PGC-1α (sc-13067) from Santa Cruz Biotechnology (Dallas, Texas, USA), anti-β-actin (A5441) from Sigma Aldrich, and anti-GAPDH (2118) from Cell Signaling Technology (Danvers, MA, USA). Horse radish peroxidase-conjugated mouse and rabbit secondary antibodies were used for detection of protein bands. The antigen-antibody binding was detected using a chemiluminescent detection reagent (Bio-Rad).

2.5. Plasmid DNA Design and Transient Transfection:

The promoter region of mouse PLIN5 from -1883 to +93 was synthesized by PCR, and the band size was confirmed by running it on an agarose gel. Then, the band was extracted by gel extraction and cloned into the pGL3-basic vector, which was designated as pmPLIN5-1883/+93. In the promoter region, putative LRH-1 binding sequences were marked and deleted by site-directed mutagenesis using a Quick-change II Site-Directed Mutagenesis kit (Agilent Technologies Inc., Santa Clara, CA, USA). For transfection, HEK-293T cells were seeded on 6-well plates, and cells were transfected with pmPLIN5 with or without murine LRH-1 and pCMV-β-galactosidase expression vector. The next day, 100 μM DLPC was treated on the cells and incubated for 24 h. Finally, cells were lysed by reporter lysis buffer (Promega corporation, Madison, WI 53711 USA) and luciferase assay were performed (21).

2.6. Lipid Analysis:

For lipids extraction, livers were homogenized in 2:1 (v/v) chloroform:methanol three times followed by drying under the stream of

nitrogen gas. These dried samples were resuspended in 1:1 (v/v) chloroform:methanol and 50 mM lithium chloride (LiCl) solution, and the lower layer was collected after centrifugation at 1,400 × *g* for 10 min. To the upper layer, chloroform was added, and the samples was re-centrifuged to collect the lower layer, which was repeated twice. Samples that were collected three times were pooled together and dried in a stream of nitrogen gas. Subsequently, dried samples were processed again and resuspended in 1:1 (v/v) chloroform:methanol maintaining the concentration of LiCl to 10 mM. After centrifugation, the lower layer was collected and the above-mentioned procedure was consecutively followed to collect the dried samples. To the dried samples, chloroform was added and vortexed. Finally, TG and cholesterol were quantified by TG-S and ASAN SET total-cholesterol kit (Asan pharm. Co, Gyeonggi-do, Korea), respectively, according to the manufacturer's instructions. Lipid contents were normalized to the liver tissue weight. Similarly, serum TGs and cholesterol were analyzed using the TG-S and ASAN SET total-cholesterol kit. Serum non-esterified fatty acids (NEFA) level was determined utilizing NEFA C kit (Wako, Osaka, Japan).

2.7. Isolation and Culture of Primary Hepatocytes:

Hepatocytes were isolated from the 24 h-fasted and fed livers of WT and LRH-1 LKO mice using perfusion method (22). Initially, mice were anesthetized with isoflurane (Hana Pharm. Co., Gyeonggi-Do, Korea) and laparotomy was performed to uncover the portal vein. Then, the vein was catheterized and the liver was perfused with Earle's balanced salt solution (EBSS, Welgene Inc., Gyeongsan, Korea) and 0.5 M EGTA to

eliminate the blood followed by 40 μg/ml liberase perfusion (Roche Diagnostics, Indianapolis, IN, USA) containing EBSS and 2 M $CaCl_2 \cdot H_2O$. Next, the liver was instantly detached to a 10-cm culture dish and gently minced with EBSS and 2 M $CaCl_2 \cdot H_2O$. Next, cells were filtered through a 100-μm nylon cell strainer to remove tissue debris followed by centrifugation of the filtrate at 50 × *g* for 1 min at 4 ℃. Subsequently, the pellet was re-suspended in percoll buffer (GE Healthcare) and re-centrifuged at 100 × *g* for 10 min at 4 ℃ to collect the viable hepatocytes in the pellet. Finally, cell pellet was gently resuspended in William's Medium E (Gibco) supplemented with 10% FBS, 1% Glutamax and 100 U/ml P/S and successively plated the cells on collagen-coated culture dishes for 3−4 h.

2.8. Lipid Droplets Staining:

For marking LDs by Oil red-O, WT and LRH-1 LKO mice were sacrificed after feeding or fasting for 24 h and livers were removed instantly. The liver samples were cut into 10-μm sections and fixed with 4% paraformaldehyde for 10 min at room temperature. Similarly, for staining lipid droplets via boron-dipyrromethene (BODIPY, Invitrogen), primary hepatocytes isolated from WT and LRH-1 LKO mice were seeded on 8-well chamber. Cells were grown overnight either in fed (DMEM, 10% FBS, 1% P/S) or in fasting (DMEM, 2% LPDS, 1% P/S) media. The next day, hepatocytes were washed with DPBS buffer (Welgene) and fixed with 4% paraformaldehyde for 10 min at room temperature. Then, cells were treated with blocking solution (1% BSA in DPBS) for 30 min followed by overnight incubation with PLIN5 antibody (NB110-60509, Novus Biologicals, Centennial, CO, USA) at 4

℃. Next day, after washing, cells were treated with secondary antibody (Alexa Fluor 594, Invitrogen) and incubated for 1 h in the dark at room temperature. Subsequently, cells were stained with 2 μM BODIPY^{TM} (493/503) (Invitrogen) and incubated for 10 min at room temperature. Finally, cells were washed with DPBS buffer and covered with mounting medium, and then observed using confocal laser scanning microscopy (Leica Microsystems, Wetzlar, Germany).

2.9. Chromatin-immunoprecipitation (ChIP) Assay:

Chromatin was prepared from liver tissue of WT and LRH-1 LKO mice fed or fasted for 24 h (22). Liver tissues were minced and crosslinked with 1% paraformaldehyde and rotated for 8 min at room temperature. Crosslinking was stopped by adding 0.125 M glycine, and then rotated for additional 5 min at room temperature. Finally, total chromatin was extracted from liver tissues and sonicated enough to obtain DNA fragments of 500 bp to 200 bp. Next, DNA were subjected to ChIP using an anti-LRH-1 antibody (sc-393369X) from Santa Cruz Biotechnology and then qPCR was performed.

2.10. Statistical Analysis:

Data were analyzed utilizing GraphPad Prism 8.4 software (GraphPad Software Inc., San Diego, CA, USA). Data are presented as mean ± SEM. Statistical differences between groups were analyzed using two-tailed student's t-test. Differences value less than $p < 0.05$ were declared significant.

Table 1. Primer Sequences for qPCR

Primer name		Sequences (5′→3′)
Mouse		
L32	sense	ACATTTGCCCTGAATGTGGT
	antisense	ATCCTCTTGCCCTGATCCTT
Lrh-1	sense	TCATGCTGCCCAAAGTGGAGA
	antisense	TGGTTTTGGACAGTTCGCTT
Plin5	sense	TGTCCAGTGCTTACAACTCGG
	antisense	CAGGGCACAGGTAGTCACAC
Pparα	sense	AGAGCCCCATCTGTCCTCTC
	antisense	ACTGGTAGTCTGCAAAACCAAA
Cyp8b1	sense	CAAAGCCCCAGCGCCT
	antisense	TTCGACTTCAAGCTGGTCGA
Cpt1-α	sense	CTCCGCCTGAGCCATGAAG
	antisense	CACCAGTGATGATGCCATTCT
Fgf21	sense	CTGCTGGGGGTCTACCAAG
	antisense	CTGCGCCTACCACTGTTCC
Mttp	sense	CTCTTGGCAGTGCTTTTTCTCT
	antisense	GAGCTTGTATAGCCGCTCATT
ApoB	sense	TTGGCAAACTGCATAGCATCC

	antisense	TCAAATTGGGACTCTCCTTTAGC
Human		
RPLP0	sense	GTGCTGATGGGCAAGAAC
	antisense	AGGTCCTCCTTGGTGAAC
LRH-1	sense	CTTTGTCCCGTGTGTGGAGAT
	antisense	GTCGGCCCTTACAGCTTCTA
PLIN5	sense	AGGCTGACGCAGAAGAATTG
	antisense	AACAGAAGGCATTGGGCAAA

ApoB: apolipoprotein B; *Cpt-1α*: carnitine palmitoyltransferase 1 alpha; *Cyp8b1*: cytochrome p450 8b1; *Fgf21*: fibroblast growth factor 21; *Lrh-1*: liver receptor homolog-1; *L32*: ribosomal protein L32; *Mttp*: microsomal triglyceride transfer protein; *Plin5*: perilipin 5; *Pparα*: peroxisome proliferator-activated receptor alpha; *RPLP0*: ribosomal protein lateral stalk subunit P0.

3. Results

3.1. LRH-1 Mitigates Hepatic Lipid Overload:

To understand the function of LRH-1 in regulating TGs during nutrient deprivation state, WT and LRH-1 LKO mice were either fed or fasted for 24 h and the liver (Figure 1A) and serum were isolated to examine the hepatic and serum TGs levels. Initially, LRH-1 LKO livers fasted for 24 h displayed higher accumulation of lipids compared to that of fasted WT livers in Oil red-O staining (Figure 1B). Furthermore, quantification of staining also confirmed an increase in lipid levels in LRH-1 LKO liver (Figure 1C), implying the necessity of further analysis of lipid levels in the liver and serum. Interestingly, fasted LRH-1 LKO mice exhibited remarkably escalated hepatic TGs levels compared to fasted WT mice (Figure 2A). However, there was no significant difference between the fed mice of either genotype. In contrast, hepatic cholesterol did not altered between the genotypes in either fed or fasted conditions (Figure 2B). Surprisingly, LRH-1 LKO mice either fed or fasted depicted notable decrease in serum TGs level compared to WT mice (Figure 2C). However, serum cholesterol and NEFA levels were not altered significantly (Figure 2D&E). These findings suggest that loss of LRH-1 buildup lipids in the liver indicating that LRH-1 might be a key regulator in balancing the hepatic lipid content.

3.2. LRH-1 Induces Expression of PLIN5 and Fatty Acid Oxidation-Related Genes:

To discover new potent target genes of LRH-1 involved in lipid metabolism, the mRNA and protein expression of various genes was examined in liver samples of either fed or fasted WT and LRH-1 LKO mice. The expression levels of *Lrh-1* and its target genes were measured to confirm LRH-1 LKO. As expected, the expression level of *Lrh-1* (Figure 3A) and its target genes (Figure 3B&C) were highly reduced in LRH-1 LKO livers. Moreover, fasting increased the mRNA expression of *Lrh-1* in the WT mice (Figure 3A). The expression of *Pparα*, an indicator of fasting state (23) was also enhanced in the fasted WT mice (Figure 3B).

Lipid analysis suggests LRH-1 to be the key player in lipid metabolism, which functions by diminishing the TGs content in the liver. In the liver, PLIN5 is familiar to regulate lipid metabolism (10) by promoting or inhibiting the hydrolysis of LDs (24). Therefore, the mRNA and protein expression of PLIN5 was measured. Interestingly, as *Lrh-1* expression was augmented, the *Plin5* level was also increased in the livers of WT fasted mice. However, the expression of *Plin5* was diminished pronouncedly in either fed or fasted LRH-1 LKO liver (Figure 3D).

Additionally, TGs and β-oxidation are strongly interconnected in the lipid metabolism. To understand the different liver phenotypes in WT and LRH-1 LKO mice, the expression of genes involved in fatty acid β-oxidation was measured. *Cpt-1α*, a regulator of fatty acid β-oxidation (25) depicted remarkable lower expression levels in either fed or fasted LRH-1 LKO mice. Nevertheless, expression of *Cpt-1α* was highly escalated in WT fasted mice (Figure 3E). *Fgf21*, an oxidation enhancer and lipogenesis inhibitor (26) also followed the similar trend. Either fed or fasted LRH-1 LKO mice showed significantly diminished *Fgf21* expression levels whereas fasted WT mice increased the expression of

Fgf21 (Figure 3F).

Moreover, protein levels of key genes were measured (Figure 4A). LRH-1 LKO mice either fed or fasted showed remarkable decreases in LRH-1 and PLIN5 protein levels (Figure 4A&B). These findings suggest that PLIN5 is a putative target of LRH-1 and that the loss of LRH-1 results in a decline in β-oxidation-related genes.

3.3. Putative LRH-1 Binding Regions in PLIN5 Promoter Region:

In an endeavor to discover a potent LRH-1-regulated genes, the LRH-1-binding regions in the PLIN5 promoter sequence were analyzed by ChIP sequencing (ChIP-Seq) analysis using a published mouse ChIP-seq data set for LRH-1 (1). As expected, the ChIP-Seq analysis of PLIN5 exhibited the LRH-1 binding peaks in the promoter region (Figure 5A). Furthermore, PLIN5 proximal promoter sequences were mapped utilizing the University of California Santa Cruz genome browser to identify the LRH-1 binding sites. The PLIN5 promoter region discloses four putative LRH-1-binding regions with direct orientations (-112/-106, -719/-713, -976/-970 and -1620/-1614 from the transcription starting site) (Figure 5B).

3.4. An LRH-1 Agonist Amplifies PLIN5 Gene Expression:

To determine whether PLIN5 is regulated by LRH-1 agonist, human cultured HepG2 cells were treated with 100 μM DLPC for 24 h and measured the gene expression of *LRH-1* (Figure 6A). In the presence of

DLPC, considerable elevation of mRNA expression of *PLIN5* was observed (Figure 6B). Moreover, DLPC treatment significantly increased PLIN5 protein levels (Figure 6C&E). However, LRH-1 protein levels was unaltered in DLPC treatment (Figure 6D). These observations indicate that PLIN5 could be regulated by an exogenous agonist of LRH-1, implying that LRH-1 guides PLIN5.

3.5. PLIN5 Promoter Activity is Stimulated by LRH-1:

To confirm whether LRH-1 controls PLIN5 at a transcriptional level by binding the PLIN5 promoter, the PLIN5 promoter region was cloned in the upstream site of the luciferase expression reporter gene (Figure 7A). The PLIN5 promoter design was co-transfected with or without LRH-1 expression plasmid and 100 μM DLPC. The PLIN5 promoter activity increased significantly in the presence of LRH-1 expression vector and DLPC (Figure 7B). In addition, to distinguish the main LRH-1-binding sites among the four putative sites in the PLIN5 promoter, each putative LRH-1-binding site was deleted from the construct. The deletion at the putative site -1620/-1614 diminished the luciferase activity in response to LRH-1 in comparison to that with other sites (Figure 7C).

This finding shows that -1620/-1614 in the PLIN5 promoter region was the conserved site for LRH-1 binding and its removal in the construct diminished the response to LRH-1 (Figure 8A). Furthermore, binding of the LRH-1 at the site -1620/-1614 was ratified by ChIP assay performed in the liver sample of 24 h-fasted and fed WT and LRH-1 LKO mice. When the samples were pooled down by LRH-1 antibody, the enrichment of LRH-1 binding site -1620/-1614 was

markedly elevated in livers of fasted WT mice compared to that in fed WT mice. In contrast, LRH-1 LKO liver either fed or fasted declined the enrichment. Moreover, there were significant differences between the genotypes in either fed or fasted mice (Figure 8B). These results suggested that the -1620/-1614 site in the PLIN5 promoter region is accountable for the transcriptional level regulation of PLIN5 by LRH-1.

3.6. LRH-1 Controls PLIN5 to Regulate LDs in Mouse Hepatocytes during Nutritional Stress :

To evaluate the regulation of LDs via LRH-1, primary hepatocytes were isolated from WT and LRH-1 LKO mice to perform BODIPY staining. Primary hepatocytes were grown either in complete or fasting media to understand the regulatory mechanism of LRH-1 during nutrient deprivation state in the liver. In the fasting media, PLIN5 surrounding the LDs was more abundant in the WT hepatocytes compared to the LRH-1 LKO hepatocytes. Moreover, during fasting conditions, BODIPY staining clearly exhibited escalated quantity of LDs in LRH-1 LKO hepatocytes relative to that in WT hepatocytes. Nevertheless, the sizes of the LDs in hepatocytes were found to be distinct and increased in WT fasted mice compared to that in LRH-1 LKO mice (Figure 9A). Additionally, the co-localization of PLIN5 with LDs was quantified, which correlated with the aforementioned conclusion. The co-localization of PLIN5 in LDs was increased in WT fasting media compared to that in complete media (Figure 9B).

Next, to verify alterations of the lipid quantity in the liver and serum, the mRNA expression of microsomal triglyceride transfer protein (*Mttp*), a key gene responsible for assembly and release of lipoproteins was

measured. The LRH-1 LKO mice either fed or fasted showed remarkably dropped *Mttp* mRNA expression compared to that in WT mice (Figure 9C). Furthermore, expression of the apolipoprotein B (*ApoB*) gene, a principal component present in very low density lipoproteins (VLDLs) was measured. However, the result did not expose significant differences between the genotypes (Figure 9D). Taken together, loss of LRH-1 decreases the PLIN5 co-localization in the LDs. Moreover, LRH-1 deficiency increases TGs in the liver by decreasing TGs secretion, leading to surplus in the LDs.

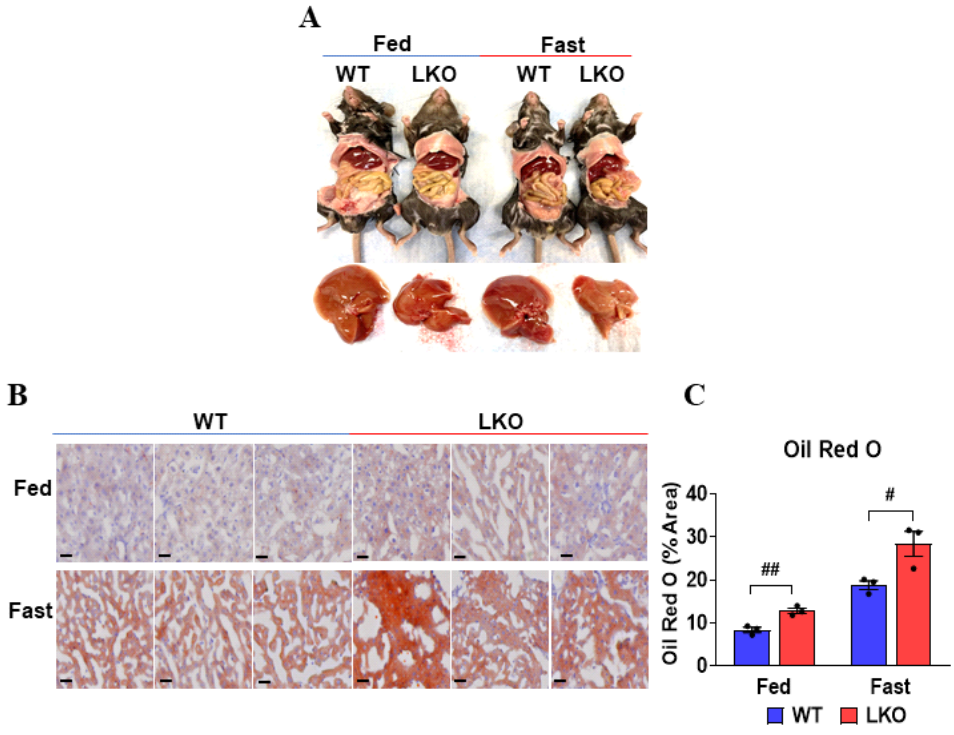

Figure 1. Loss of liver receptor homomolg (LRH)-1 increases triglycerides accumulation in the liver. (A) Dissection image of 24 h-fasted or fed WT and LRH-1 LKO mice along with their isolated livers. (B) Oil red-O staining of liver tissue (scale bar = 30 μm). (C) Quantification of staining in % area shown in B. $^{\#}p < 0.05$ and $^{\#\#}p < 0.01$, WT vs LKO. WT: wild type; LKO: liver-specific knockout.

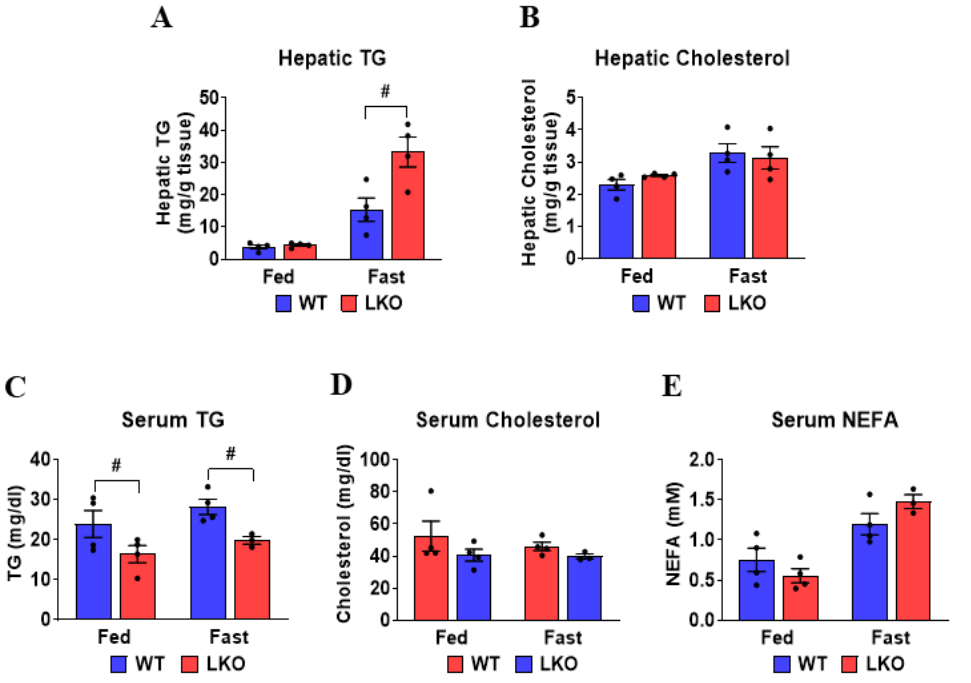

Figure 2. LRH-1 deficiency increases liver triglycerides levels and decreases serum triglycerides levels. (A) Hepatic triglycerides levels. (B) Hepatic cholesterol levels. (C) Serum triglycerides levels. (D) Serum cholesterol levels. (E) Serum NEFA levels. $^{\#}p < 0.05$, WT vs LKO. TG: triglyceride; NEFA: non-esterified fatty acids.

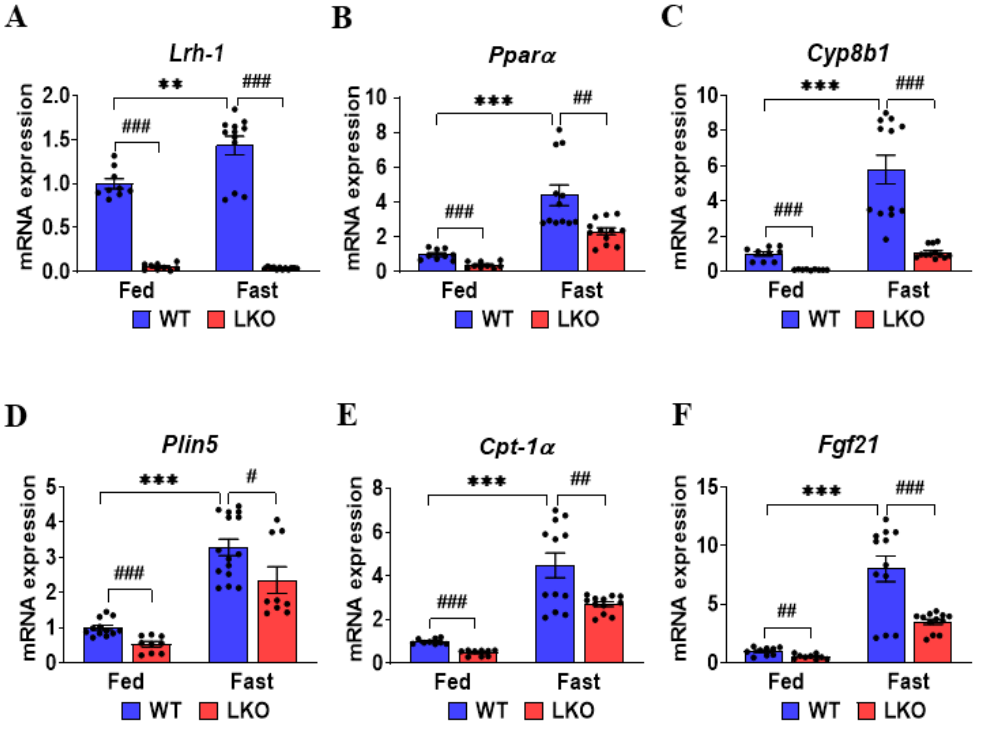

Figure 3. LRH-1 regulates perilipin 5 (PLIN5) gene and β-oxidation. All results were examined in 24 h-fasted and fed liver samples. (A) mRNA expression levels of *Lrh-1*. (B&C) mRNA expression levels of LRH-1 target genes. (D) mRNA expression levels of *Plin5*. (E) mRNA expression of *Cpt-1α*. (F) mRNA expression of *Fgf21*. $^{\#}p < 0.05$, $^{\#\#}p < 0.01$ and $^{\#\#\#}p < 0.001$, WT vs. LKO, $^{**}p < 0.01$ and $^{***}p < 0.001$, WT fed vs. WT fast. *Cpt-1α*: carnitine palmitoyltransferase 1 alpha; *Cyp8b1*: cytochrome p450 8b1; *Fgf21*: fibroblast growth factor 21; *Pparα*: peroxisome proliferator-activated receptor alpha.

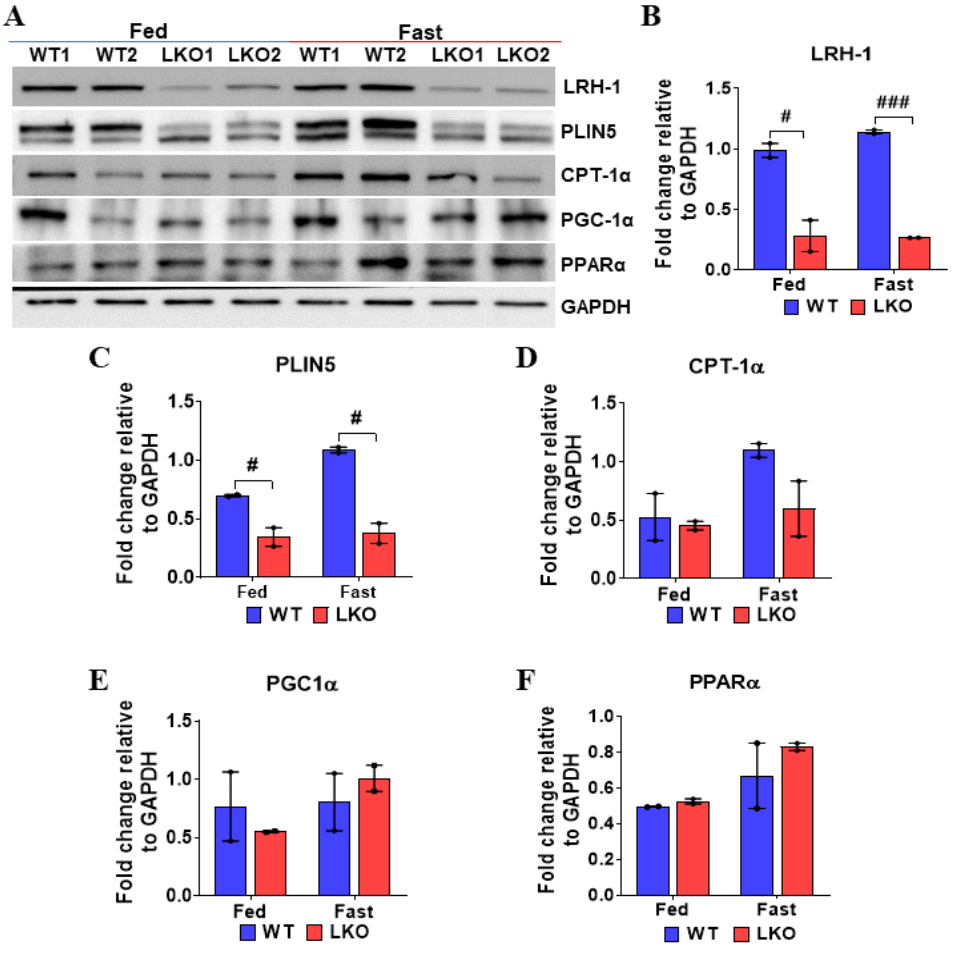

Figure 4. LRH-1 knockout liver decreases PLIN5 protein levels. All results were examined in 24 h-fasted and fed livers. (A) Western blot for protein analysis. GAPDH was used as a loading control. (B&C) Quantification of LRH-1 and PLIN5 protein levels. (D) Quantification of CPT-1α protein levels. (E&F) Quantification of PGC-1α and PPARα protein levels. $^{\#}p < 0.05$ and $^{\#\#\#}p < 0.001$, WT vs. LKO. GAPDH: glyceraldehyde-3-phosphate dehydrogenase; PGC-1α: peroxisome proliferator-activated receptor gamma coactivator 1-alpha.

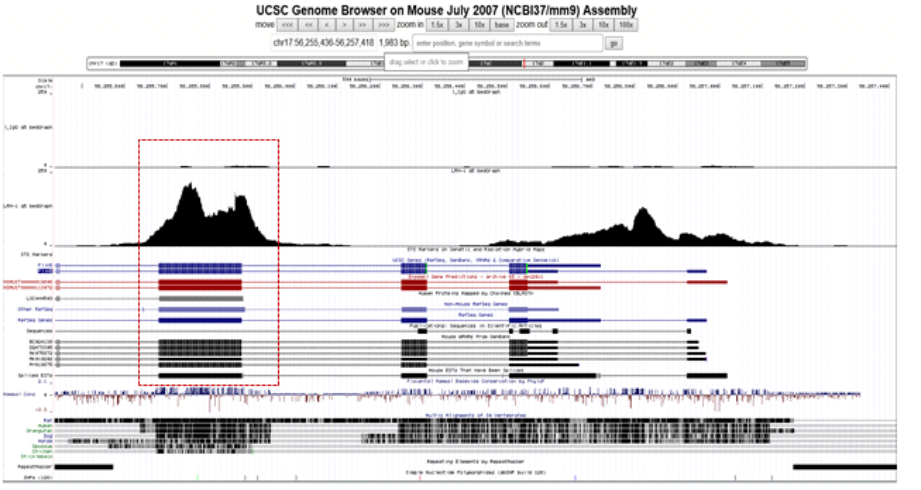

B

-1883 CCCACCCTCTGCCTTATGTTTTAAGACAGGATCTCTGGCCGGGCGGTGGTGGCGCATGCCTTTGATCCCAGCACTTGGGAGGCAGA -1798
-1797 GGCAGGTGGATTTCTGAGTTCGAGGCCAGCCTGGTCTACAGAGTGAGTTGCAGGACAGCCAGGGCTACACAGAGAAACCCTGTCT -1713
-1712 CGGGAAAATAAATAAATAAAAAATCTCTGACTGGCCAGCTGAGAGCCTCGGGATCTTTCTGCCTCTTTCTCTGCCTCTGCCTCCCAG -1626
-1625 AGCTGAGGTCACACACATGAGCCAGTGTCACACATGACAAATGTGTCAAATTGAGGTCTTCCGGCTTACATGATAAGTGATAAGCA -1540
-1539 CTTTACTGACAGTGACTGCTCTCCAGATCCTTCCCACTGTATAGCCCTGACTCTCCTGGAACTTGCTCTGTAAGCTGGCTGGTCTCAA -1452
-1451 AGTCAGAGGTCCTCCTGCCTCTACCTCCTGAGTGCTGGGATTAAAGTCCTGCATCACAACCCAGCTTTAGTTTTTTTCACCCCCTAG -1365
-1364 ACAGAGGGACTCTGCCCATTGAGAGGCAGGGGTGTGGATTTTTTTTTTAAAGGCCCGGTTTCATATTGCCCAGGCTGGCCTCAAATT -1278
-1277 TGCTATAAGCCTAGGGTGATTTGAGCTCATGATTCTCCTGTCTCCACCTTGTGGCTCTGGGTGACAAGCATATGACTGGGCAAAACT -1191
-1190 AGGCTTCTCACCCCAGTCCTGCAGAGGGAGCTGGGGAGAGTGGGTTAAAACTTGGGTCTCAGTTTGCTGATCTGTAAAATGGGGTC -1105
-1104 AGAACTGACAGGCTTAACAGCTCTCAGGATTAAACAGCAGATTAAAAATAAGATGGAGGCCAGAGAGACCACCCATGGCTTAACA -1020
-1019 GCTCAGGCTGGAGTTCCAGTCCCAGCATCCACATGATAGCTCAAGGTCACATGTTACTCCAGTCACAGGGGGTCTGTCAACTTTACT -933
-932 GGCCTCTGTGGGGATCAGGCATCTGTGGATCATGACAGATGGAACATATCAACAAAACACCAGGACACATAGACGTAATAATAAT -848
-847 AATAACAAAGGAAGTGGGCCTCAGAAGGCAGTCAGCCGAGCACCCACAGATCTGGGTTCACGCCCAGCACCACATAAACATGTGT -763
-762 GGTGTGGCACATCTGTTGTCTTAGCCACTGGGTGGTGCGTTCAAGGTCATCCTTGGCTATGTGGTTACTTTGAGGCTATCCTGGGCT -676
-675 ATATAGTGAGTTCTGGTCAAGTCTTGACTACAGAGAGAGAGTCTGAATCAAACAAAACAAACGGAAAAGACTGAAGAATGAGAA -592
-591 AGTCGCCGGGCGTGGTGGCTCATGCCTTTAATCCCAGCACTTGGGAGGCAGAGGCAAGGTGGATTTCTGAGTTCGAGGCCAACCTG -506
-505 ATCTACAAAATGAGTTCCAGGATAGCCAGAGAAAACCTGTCACAAAAAACAAAACAAAACAAAACAAAAAAAAAACACAACAAAG -422
-421 AAGAAGGAGGAGGAGGAGGAGAAAAAAGGAGGAGGAGAAAAAAGAGGAGAAGGAGAAGGAGAAGGAGAAGGAGAAGGAGAA -341
-340 GGAGAAGGAGAAAGAAGAAGAAAAGTCCTCAGTCGCCGGGCGGATTTCTGAGTTCGAGGCCAGCCTGTTCGGTCTACAGAGTGAG -256
-255 TTCCAGGACAGCCAGAGCGATACAGAGAAACCCTGTCTCGAAAAAACCAACCAACCAACCAACCAACCAAAAACCAACCAACCAACCA -172
-171 ACCAACCAATCAAACAAACAAACAACAACAACAAAAAGAAAGTCCTCAGTCCTAGTCTGAGGTCAGCCATGGTGACTGGACCAGG -87
-86 ATTCAGCGTCCCTGAGCCGCTATGGCAACCATGGCGCCTGTGGGGGGCGGGGAAGCTCCAGATCCACCCCCGGCGGCGCCTCATTG -1

Figure 5. Predicted LRH-1 binding sites on mouse PLIN5 gene. (A) LRH-1 binding regions on the liver chromosome were obtained from the LRH-1 ChIP-Seq data. (B) PLIN5 promoter sequence from -1 to -1883 from the transcriptional start site (+1). Arrows designates putative LRH-1 binding sites. ChIP-Seq: chromatin immunoprecipitation sequencing.

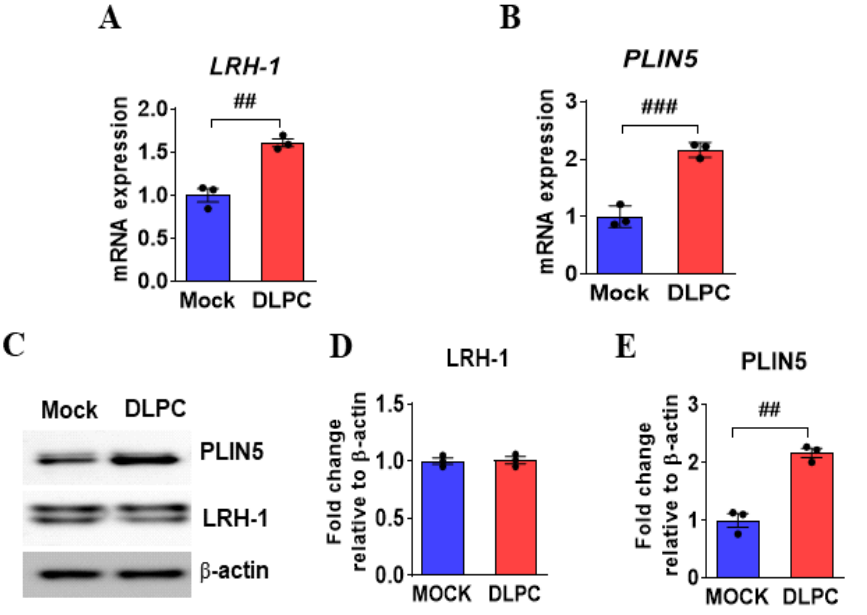

Figure 6. LRH-1 agonist increases PLIN5 gene expression. Experiment was performed in HepG2 cells by treatment with 100 μM DLPC for 24 h. (A) Expression of *LRH-1* gene after DLPC treatment. (B) Expression of *PLIN5* gene after DLPC treatment. (C) Western blot for protein analysis of PLIN5 and LRH-1 after DLPC treatment. (D&E) LRH-1 and PLIN5 protein fold change relative to β-actin which was used as a loading control. $^{\#\#}p < 0.01$ and $^{\#\#\#}p < 0.001$, Mock vs. DLPC. DLPC: dialauroylphosphatidylcholine.

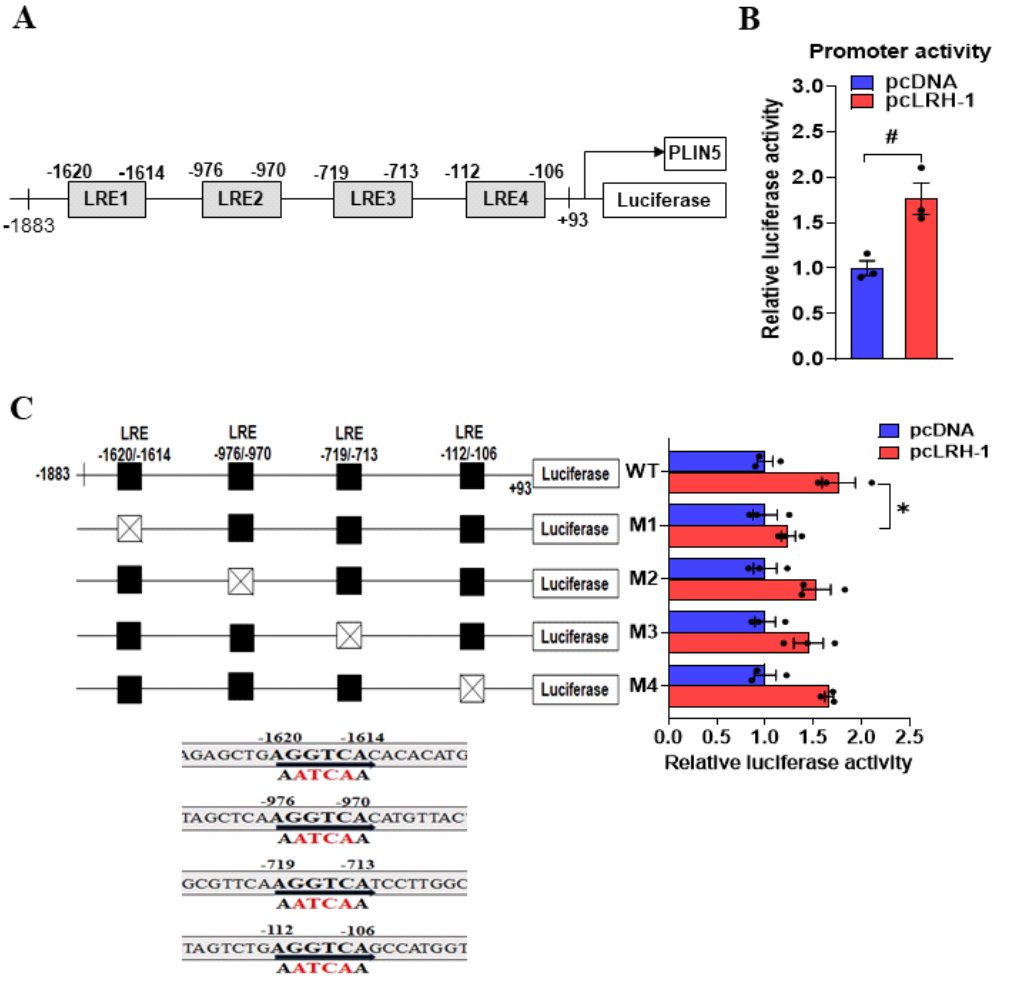

Figure 7. LRH-1 stimulates PLIN5 promoter activity. (A) Representation of putative LRH-1 binding sites in PLIN5 promoter region. (B) HEK-293T cells were transfected with pmPLIN5 containing the PLIN5 promoter upstream of the luciferase reporter gene along with a pcDNA or pcLRH-1 expression vector. (C) LRH-1 deletion mutants from the PLIN5 promoter region co-transfected with pcDNA or LRH-1 expression vector. The deleted sequences were shown in boxes. $^{\#}p < 0.05$, pcDNA vs pcLRH-1, $^{*}p < 0.05$, WT fed vs. WT fast.

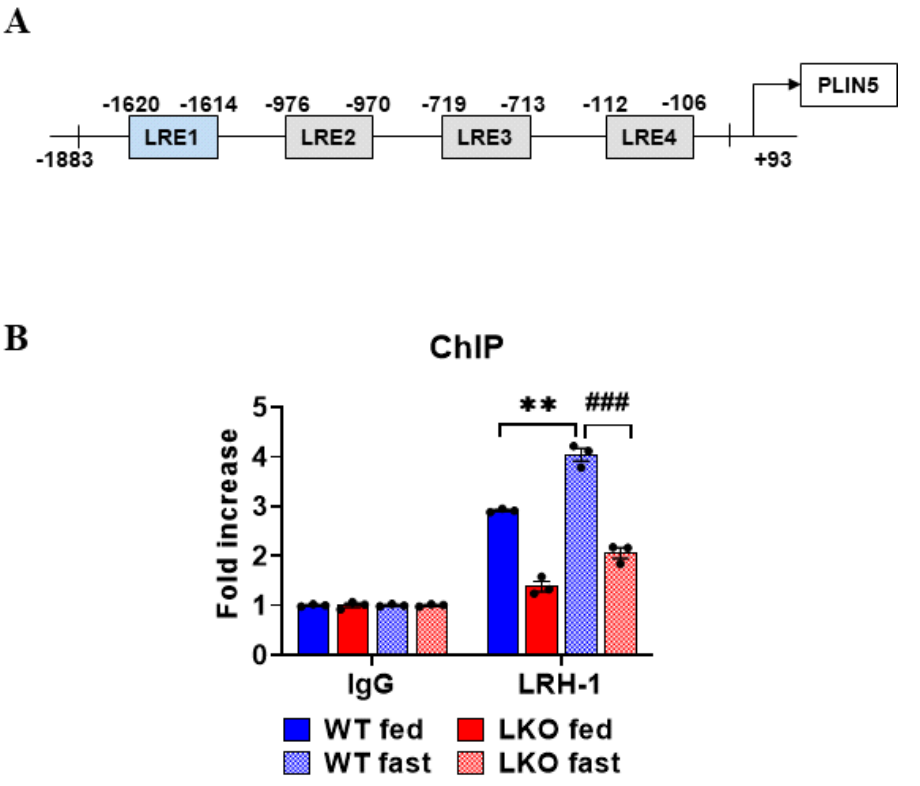

Figure 8. Chromatin immunoprecipitation assay. LRH-1 stimulates PLIN5 promoter activity by binding between the -1620 and -1614 promoter region. (A) Representation of main LRH-1 binding site in PLIN5 promoter region. (B) ChIP assay measured in 24 h-fasted or fed WT and LRH-1 LKO liver samples. $^{###}p < 0.001$, WT vs. LKO, $^{**}p < 0.01$, WT fed vs. WT fast. ChIP: chromatin immunoprecipitation.

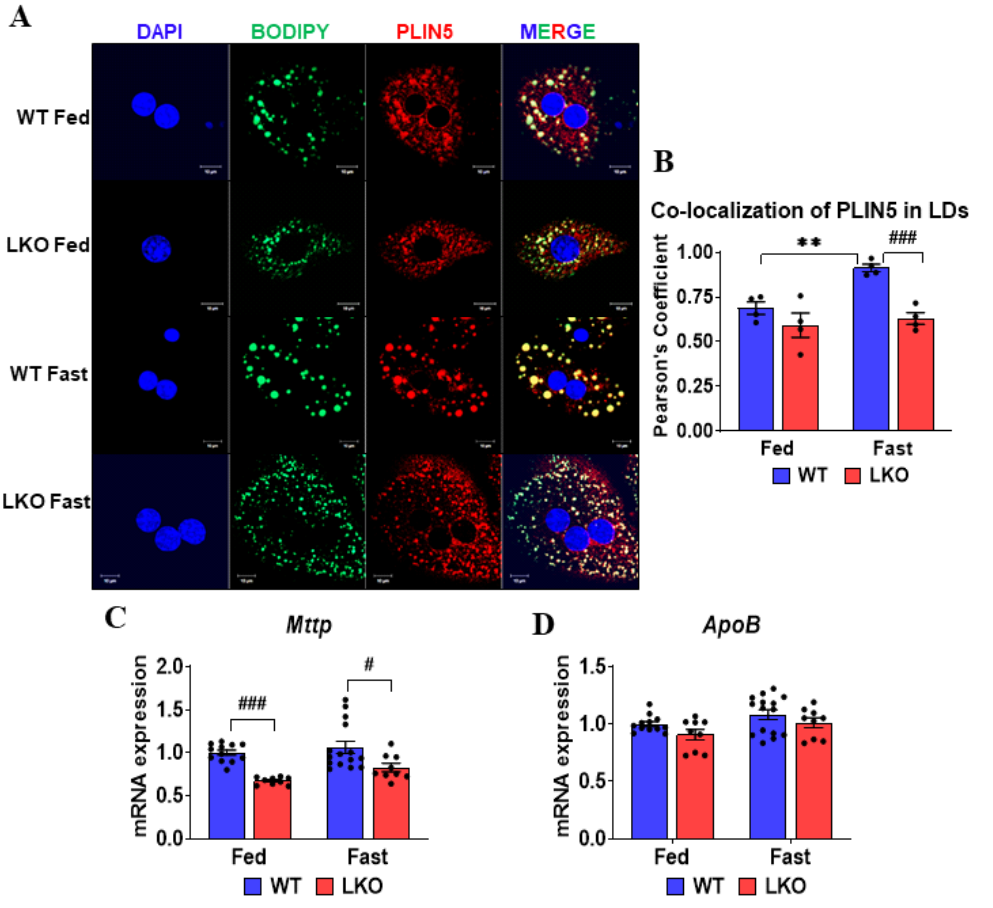

Figure 9. LRH-1 controls PLIN5 and mobilizes the lipid droplets. (A) BODIPY staining in primary hepatocytes grown in fast or complete media followed by overnight incubation of PLIN5 antibody. (B) Co-localization of PLIN5 in LDs shown in figure A. (C&D) mRNA expression of genes related to VLDL secretion measured in 24 h-fasted or fed livers. All data are shown as the mean ± SEM. $^{\#}p < 0.05$ and $^{\#\#\#}p < 0.001$, WT vs. LKO, $^{**}p < 0.01$, WT fed vs. WT fast. *ApoB*: apolipoprotein B; LDs: lipid droplets; *Mttp*: microsomal triglyceride transfer protein; VLDL: very low density lipoproteins.

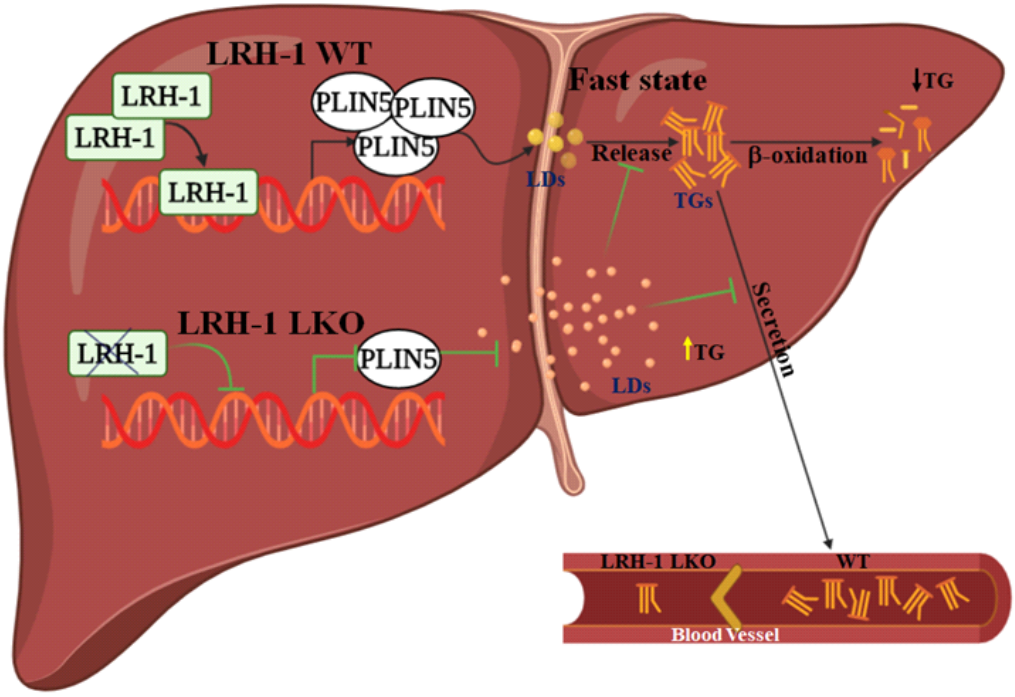

Figure 10. Scheme illustrating the role of LRH-1 in the liver during fasting state. LRH-1 regulates PLIN5 gene expression and mobilizes triglycerides in the liver during nutritional stress. Deletion of LRH-1 increases the triglycerides in the liver during fasting by lowering the β-oxidation and triglycerides secretion.

4. Discussion

Hepatic LRH-1 is a transcriptional regulator of glucose metabolism and bile acid homeostasis (27). This study discovered PLIN5 as a direct target of LRH-1 and explored the function of LRH-1 in the liver during a nutritional deprivation state. Prolonged fasting is well known to accumulate hepatic TGs (28). In this study, fasting increased the accumulation of liver TGs more readily in the livers of LRH-1 LKO mice compared to that in WT livers. The elevation of hepatic TGs in the liver might be due to decrease in β-oxidation. As expected, livers of LRH-1 LKO mice either fed or fasted depicited the highly diminished expression of key gene responsible for β-oxidation as well as their enhancer gene. These findings indicate the possibilities for accumulation of lipids in the liver. Recent studies on LRH-1 LKO mouse revealed that LRH-1 promotes β-oxidation and mitochondrial biogenesis (8). Incidentally, this result coincides with the previous findings in PLIN5 LKO mice (10), demonstrating elevated hepatic TGs levels and a reduction in fatty acid oxidation in the liver. However, these findings were in contrast with the reported research performed by Wang et al. (28). They reported decreased TGs in the liver and increased β-oxidation in whole-body PLIN5 KO mice. Together, this suggests close phenotypic similarity between LRH-1 and PLIN5 due to transcriptional regulation of PLIN5 by LRH-1.

Interestingly, fasted LRH-1 LKO mice exhibited a decrease in serum TGs level compared to that in WT mice. The alteration of the liver and serum TGs levels between the genotypes were observed, which might be due to the decrease in TGs secretion from the liver (29). Therefore, the genes involved in VLDL secretion from the liver were measured.

The gene expression of *Mttp*, a key player in VLDL secretion was markedly decreased in LRH-1 LKO livers, however *ApoB* was unaltered. Moreover, the activation of *Pparα* in the liver enhances the expression of *Mttp* gene (30) and it is reported that *Pparα* also activates *Plin5* in the liver (31). Furthermore, a decrease in TGs secretion was reported in PLIN5 LKO mice (10). Collectively, these data suggest that MTTP might be responsible for decreasing serum TGs in the liver of LRH-1 LKO mice.

Transcription factors often bind and sense lipid molecules (32). LRH-1 binds to the-1620/-1614 binding sequence in the PLIN5 promoter region for the transcriptional regulation of PLIN5 which was confirmed by promoter activity and ChIP assays. In addition, DLPC as an agonist of LRH-1, which has previously established role in the synthesis of bile acids and reduction in hepatic TGs (33) increases the mRNA expression of *Plin5*. Therefore, these findings indicate that LRH-1 regulates PLIN5 in the transcriptional level.

PLIN5 balances fatty acid requirements to meet cellular necessity, protecting mitochondria during extreme fatty acid flux in low-energy demands and encouraging fatty acid mobilization and oxidation in high-energy demands (34). In the BODIPY staining, fasted WT hepatocytes demonstrated the utilization of LDs, whereas lipids were piled up in the fasted LRH-1 LKO hepatocytes. Furthermore, PLIN5 and BODIPY staining clearly displayed more intense red and green fluorescence respectively, implying the co-localization of PLIN5 in LDs during fasting in WT hepatocytes. This indicates that the loss of LRH-1 decreases the PLIN5 co-localization in LDs and increases lipid content. Interestingly, in the fasted WT hepatocytes, the size of the LDs was increased and distinct compared to that in fasted LRH-1 LKO hepatocytes. However, the quantity of lipids was increased in the fasted

LRH-1 KO hepatocytes. A previous result reported a decrease in the amount and size of the LDs in whole body PLIN5 KO mice (28). However, in this study, the amount of LDs increased in the LRH-1 LKO mice. PLIN5 regulates both the storage and usage of TGs, which is regarded as metabolically protective (35). In fasted WT hepatocytes, the presence of LRH-1 regulates PLIN5 to protect the liver by increasing the influx of TGs within the LDs. As a result, this increases size of LDs. In addition, it promotes fatty acid oxidation to meet the cellular energy demand during fasting, resulting in reduced number of LDs. In contrast, the lack of LRH-1 in the LRH-1 LKO mice attenuated PLIN5 expression that resulted in small-sized LDs but increased their numbers. This might be the mechanism underlying the changes in size and quantity of LDs, respectively. Overall, these observations indicate that LRH-1 regulates PLIN5 to mobilize LDs and balances hepatic lipid contents.

In summary, this study uncovered the function of LRH-1 in the liver during nutrient deprivation state and presents the novel target of LRH-1 in the liver. It concludes the necessity of LRH-1 in lipid management to protect the liver from lipid accumulation. In the liver, LRH-1 regulates PLIN5 to mobilize the lipids and maintains this balance during nutritional stress situation (Figure 10). Additionally, LRH-1 regulates PLIN5 to equilibrate the cellular needs and storage of lipids, thus defending the liver from metabolic diseases associated with fatty liver. Although LRH-1 is involved in managing the lipid content in the liver, further studies are required to assess the possibilities for the treatment of nonalcoholic steatohepatitis. Thus, this study might be a platform to elucidate the underlying mechanism for the treatment of nonalcoholic steatohepatitis.

5. Summary

LRH-1 is an orphan nuclear receptor highly expressed in the liver. It regulates the genes involved in bile acid homeostasis and glucose metabolism. However, the role of LRH-1 in lipid metabolism during nutrient stress conditions is not fully addressed. This study explored the function of LRH-1 during nutrient deprivation condition as well as identified the novel target gene of LRH-1 in the liver. The findings revealed that LRH-1 regulates the PLIN5 gene expression in the liver. During nutritional stress conditions like fasting, the level of TGs enhanced and the LRH-1 regulates the PLIN5 gene expression in the liver. It also promoted fatty acid oxidation to meet the cellular energy demand as well as increased TGs secretion in the bloodstream to lower the hepatic lipid contents. However, LRH-1 LKO liver attenuated the fatty acid oxidation as well as TGs secretion in the blood, resulting in increased hepatic lipid contents. These results provide strong evidence for describing the role of LRH-1 in the hepatic lipid metabolism during nutritional stress situation.

References

1. Chong HK, Biesinger J, Seo YK, Xie X, Osborne TF: Genome-wide analysis of hepatic LRH-1 reveals a promoter binding preference and suggests a role in regulating genes of lipid metabolism in concert with FXR. BMC Genomics 2012; 13: 51.

2. Fayard E, Auwerx J, Schoonjans K: LRH-1: an orphan nuclear receptor involved in development, metabolism and steroidogenesis. Trends Cell Biol 2004; 14: 250-60.

3. Stein S, Lemos V, Xu P, Demagny H, Wang X, Ryu D, et al.: Impaired SUMOylation of nuclear receptor LRH-1 promotes nonalcoholic fatty liver disease. J Clin Invest 2017; 127: 583-92.

4. Schwaderer J, Phan TS, Glockner A, Delp J, Leist M, Brunner T, et al.: Pharmacological LRH-1/Nr5a2 inhibition limits pro-inflammatory cytokine production in macrophages and associated experimental hepatitis. Cell Death Dis 2020; 11: 154.

5. Holmstrom SR, Deering T, Swift GH, Poelwijk FJ, Mangelsdorf DJ, Kliewer SA, et al.: LRH-1 and PTF1-L coregulate an exocrine pancreas-specific transcriptional network for digestive function. Genes Dev 2011; 25: 1674-9.

6. Duggavathi R, Volle DH, Mataki C, Antal MC, Messaddeq N, Auwerx J, et al.: Liver receptor homolog 1 is essential for ovulation. Genes Dev 2008; 22: 1871-6.

7. Mueller M, Cima I, Noti M, Fuhrer A, Jakob S, Dubuquoy L, et al.: The nuclear receptor LRH-1 critically regulates extra-adrenal glucocorticoid synthesis in the intestine. J Exp Med 2006; 203: 2057-62.

8. Choi S, Dong B, Lin CJ, Heo MJ, Kim KH, Sun Z, et al.: Methyl-sensing nuclear receptor liver receptor homolog-1 regulates mitochondrial function in mouse hepatocytes. Hepatology 2020; 71: 1055-69.

9. Mamrosh JL, Lee JM, Wagner M, Stambrook PJ, Whitby RJ, Sifers RN, et al.: Nuclear receptor LRH-1/NR5A2 is required and targetable for liver endoplasmic reticulum stress resolution. Elife 2014; 3: e01694.

10. Keenan SN, Meex RC, Lo JCY, Ryan A, Nie S, Montgomery MK, et al.: Perilipin 5 deletion in hepatocytes remodels lipid metabolism and causes hepatic insulin resistance in mice. Diabetes 2019; 68: 543-55.

11. Kimmel AR, Sztalryd C: Perilipin 5, a lipid droplet protein adapted to mitochondrial energy utilization. Curr Opin Lipidol 2014; 25: 110-7.

12. Khor VK, Shen WJ, Kraemer FB: Lipid droplet metabolism. Curr Opin Clin Nutr Metab Care 2013; 16: 632-7.

13. Pol A, Gross SP, Parton RG: Review: biogenesis of the multifunctional lipid droplet: lipids, proteins, and sites. J Cell Biol 2014; 204: 635-46.

14. Langhi C, Marquart TJ, Allen RM, Baldan A: Perilipin-5 is regulated by statins and controls triglyceride contents in the hepatocyte. J Hepatol 2014; 61: 358-65.

15. Tan Y, Jin Y, Wang Q, Huang J, Wu X, Ren Z: Perilipin 5 protects against cellular oxidative stress by enhancing mitochondrial function in HepG2 cells. Cells 2019; 8: 1241.

16. Yokota S, Nakamura K, Ando M, Kamei H, Hakuno F, Takahashi S, et al.: Acetylcholinesterase (AChE) inhibition aggravates fasting-induced triglyceride accumulation in the mouse liver. FEBS Open Bio 2014; 4: 905-14.

17. Li Y, Chao X, Yang L, Lu Q, Li T, Ding WX, et al.: Impaired fasting-induced adaptive lipid droplet biogenesis in liver-specific Atg5-deficient mouse liver is mediated by persistent nuclear factor-like 2 activation. Am J Pathol 2018; 188: 1833-46.

18. Geisler CE, Hepler C, Higgins MR, Renquist BJ: Hepatic adaptations to maintain metabolic homeostasis in response to fasting and refeeding in mice. Nutr Metab (Lond) 2016; 13: 62.

19. Asimakopoulou A, Engel KM, Gassler N, Bracht T, Sitek B, Buhl EM, et al.: Deletion of perilipin 5 protects against hepatic injury in nonalcoholic fatty liver disease via missing inflammasome activation. Cells 2020; 9: 1346.

20. Gallardo-Montejano VI, Saxena G, Kusminski CM, Yang C, McAfee JL, Hahner L, et al.: Nuclear perilipin 5 integrates lipid droplet

lipolysis with PGC-1alpha/SIRT1-dependent transcriptional regulation of mitochondrial function. Nat Commun 2016; 7: 12723.

21. Lee JS, Bae S, Kang HS, Im SS, Moon YA: Liver receptor homolog-1 regulates mouse superoxide dismutase 2. Biochem Biophys Res Commun 2017; 489: 299-304.

22. Im SS, Hammond LE, Yousef L, Nugas-Selby C, Shin DJ, Seo YK, et al.: Sterol regulatory element binding protein 1a regulates hepatic fatty acid partitioning by activating acetyl coenzyme A carboxylase 2. Mol Cell Biol 2009; 29: 4864-72.

23. Inagaki T, Dutchak P, Zhao G, Ding X, Gautron L, Parameswara V, et al.: Endocrine regulation of the fasting response by PPARalpha-mediated induction of fibroblast growth factor 21. Cell Metab 2007; 5: 415-25.

24. Du J, Hou J, Feng J, Zhou H, Zhao H, Yang D, et al.: Plin5/p-Plin5 guards diabetic CMECs by regulating FFAs metabolism bidirectionally. Oxid Med Cell Longev 2019; 2019: 8690746.

25. Weber M, Mera P, Casas J, Salvador J, Rodriguez A, Alonso S, et al.: Liver CPT1A gene therapy reduces diet-induced hepatic steatosis in mice and highlights potential lipid biomarkers for human NAFLD. FASEB J 2020; 34: 11816-37.

26. Lin X, Liu YB, Hu H: Metabolic role of fibroblast growth factor 21 in liver, adipose and nervous system tissues. Biomed Rep 2017; 6: 495-502.

27. Oosterveer MH, Mataki C, Yamamoto H, Harach T, Moullan N, van Dijk TH, et al.: LRH-1-dependent glucose sensing determines intermediary metabolism in liver. J Clin Invest 2012; 122: 2817-26.

28. Wang C, Zhao Y, Gao X, Li L, Yuan Y, Liu F, et al.: Perilipin 5 improves hepatic lipotoxicity by inhibiting lipolysis. Hepatology 2015; 61: 870-82.

29. Khalil A, Cevik SE, Hung S, Kolla S, Roy MA, Suvorov A: Developmental exposure to 2,2′,4,4′-tetrabromodiphenyl ether permanently alters blood-liver balance of lipids in male mice. Front Endocrinol (Lausanne) 2018; 9: 548.

30. Ameen C, Edvardsson U, Ljungberg A, Asp L, Akerblad P, Tuneld A, et al.: Activation of peroxisome proliferator-activated receptor alpha increases the expression and activity of microsomal triglyceride transfer protein in the liver. J Biol Chem 2005; 280: 1224-9.

31. Wolins NE, Quaynor BK, Skinner JR, Tzekov A, Croce MA, Gropler MC, et al.: OXPAT/PAT-1 is a PPAR-induced lipid droplet protein that promotes fatty acid utilization. Diabetes 2006; 55: 3418-28.

32. Seitz C, Huang J, Geiselhoringer AL, Galbani-Bianchi P, Michalek S, Phan TS, et al.: The orphan nuclear receptor LRH-1/NR5a2 critically regulates T cell functions. Sci Adv 2019; 5: eaav9732.

33. Lee JM, Lee YK, Mamrosh JL, Busby SA, Griffin PR, Pathak MC, et al.: A nuclear-receptor-dependent phosphatidylcholine pathway

with antidiabetic effects. Nature 2011; 474: 506-10.

34. Mason RR, Watt MJ: Unraveling the roles of PLIN5: linking cell biology to physiology. Trends Endocrinol Metab 2015; 26: 144-52.

35. Harris LA, Skinner JR, Shew TM, Pietka TA, Abumrad NA, Wolins NE: Perilipin 5-driven lipid droplet accumulation in skeletal muscle stimulates the expression of fibroblast growth factor 21. Diabetes 2015; 64: 2757-68.

Regulation of PLIN5 Gene Expression by LRH-1 in the Liver

Pantha, Rubee

Department of Physiology
Graduate School

Keimyung University

(Supervised by Professor Im, Seung Soon)

(Abstract)

The liver receptor homolog-1 (LRH-1) has emerged as a regulator of hepatic glucose, bile acid and mitochondrial metabolism. However, the functional mechanism of LRH-1 on lipid mobilization has not been addressed. This study investigated the regulatory function of LRH-1 in lipid metabolism during fasting. The wild type (WT) and LRH-1 liver specific knockout (LKO) mice were either fed or fasted for 24 h and the liver and serum were isolated. During fasting, LRH-1 LKO mice showed greater accumulation of triglycerides in the liver compared to WT mice. Interestingly, LRH-1 LKO liver decreased the perilipin 5 (PLIN5) expression and genes involved in β-oxidation. Additionally, the LRH-1 agonist dialauroylphosphatidylcholine also enhances the PLIN5 expression in human cultured HepG2 cells. To identify new target gene of LRH-1,

these findings direct to analyze the PLIN5 promoter sequence which revealed -1620/-1614 to be a putative binding site of LRH-1. It was confirmed by promoter activity and chromatin immunoprecipitation assay. Moreover, fasted primary hepatocytes isolated from WT mice increased the co-localization of PLIN5 in lipid droplets (LDs) compared to fasted LKO primary hepatocytes. Overall, these findings suggest that PLIN5 may be a novel target of LRH-1 to mobilize the LDs and manage the cellular needs.

간에서 LRH-1에 의한 PLIN5 유전자 발현 조절

뻔터 루비
계 명 대 학 교 대 학 원
의학과 생리학 전공
(지도교수 임 승 순)

(초록)

간 수용체 동족체-1 (LRH-1)은 간에서 포도당, 담즙산 및 미토콘드리아 대사의 조절자로 알려져 있다. 그러나 지질 동원을 위한 LRH-1의 기능적 메커니즘은 잘 연구되어지지 않았다. 이 연구에서는 영양 결핍 상태에서 정상적인 간의 생리 상태를 유지하기 위해 지질 대사에 관여하는 LRH-1의 조절기능을 규명하였다. 정상 및 간 특이적 LRH-1 결핍 마우스를 식이하거나 24 시간 동안 금식하고 난 후에 간 및 혈청을 분리하였다. LRH-1의 표적인자를 규명하기 위해서 mRNA 발현 분석, 단백질의 발현 확인 및 조직병리학적 분석을 사용하였다. 먼저 일차 간세포를 분리한 후 지질의 면역염색을 수행한 결과, 금식하는 동안 결핍 마우스는 정상 마우스와 비교하여 간에서 중성지방이 더 축적됨을 확인하였다. 그리고 흥미롭게도 LRH-1이 결핍된 마우스의 간에서 perilipin 5 (PLIN5)의 발현이 감소하였고, 지방산 β-산화에 관여하는 유전자들이 감소됨을 확인하였다. 또한, LRH-1 활성물질인 dialauroylphosphatidylcholine을 처리하였을 때 인체 유래 간세포인

HepG2 세포에서 PLIN5의 발현이 증가됨을 알 수 있었다. PLIN5가 LRH-1의 새로운 표적 유전자인지를 검증하기 위해서 프로모터 분석과 염색질 면역항체침전법 분석을 통해 마우스 PLIN5 프로모터의 -1620 bp와 -1614 bp 사이에 LRH-1가 결합하는 부위가 있음을 검증하였다. 또한, 금식된 정상 마우스의 일차 간세포는 금식된 LRH-1 결핍 마우스의 일차 간세포에 비해 지질 방울에서 PLIN5가 함께 발현되는 것을 확인하였다. 결론적으로, 이 연구에서 LRH-1은 세포의 에너지 요구에 따른 지방산 베타 산화를 유도하고, 혈중으로 중성지방 분비를 증가시키며, 금식에 의한 영양 결핍 시에 지질 축적으로부터 간을 보호하는 기능을 하고 있는 중요한 조절자임을 새롭게 밝혔다.